

Water and salt transport in plaster/substrate systems

H.P. Huinink, J. Petkovic, L. Pel and K. Kopinga

Department of Applied Physics, Technische Universiteit Eindhoven, Eindhoven, The Netherlands

The transport of salt and water during drying has been studied in systems consisting of a substrate covered with either one or two plaster layers. The drying behaviour of these systems was modelled with invasion percolation (IP) algorithms. The model outcomes were compared with experimental results obtained with Nuclear Magnetic Resonance (NMR). It was found that drying behaviour of the plaster layers was strongly influenced by the properties of the substrate. When the substrate has the widest pores, the plaster layers stay wet while the substrate dries out. As a consequence most salt, present in the substrate, moves to the plaster layers and accumulates at the external surface. In the case that the substrate has the smallest pores, the plaster layers dry out first. In this case salts also crystallize in the substrate. Further we have tried to make an accumulating plaster system consisting of two layers on top of a substrate, which would function purely on the basis of differences in pore sizes between the layers. The drying behaviour in the presence of pure water was as predicted by the model. However, in the case of a salt solution the salt modified the drying behaviour such that the accumulation properties of the system were reduced. Therefore, we conclude that for transporting systems tuning the pore-sizes of the layers suffices, but for accumulating systems it seems that additives, for example water repellents, have to be used.

Key words: Plaster, transport, salt, water, crystallization

1 Introduction

Soluble salts play an important role in stone weathering processes [Evans, 1970; Goudie & Viles, 1997]. The mechanism responsible for damage by salt is still under debate [Charola, 2000]. However, it seems that both the transport and crystallization of salts are key factors in salt weathering. Both the transport and the crystallization of salts are closely linked with the evolution of the water distribution inside the stone [Pel, 2002; Huinink 2002]. When a stone contains a significant amount of liquid water, soluble salts will dissolve. During the drying of the stone, salts are transported along with the water to spots where the water evaporates. In the neighbourhood of these spots, salts will precipitate and damage the stone matrix. Many walls of ancient buildings are covered with plaster layers. When during restoration projects new plaster layers have to be applied, their compositions are chosen such that these layers could have a long lifetime and should protect the underlying stones against salt

weathering. Often it is assumed that the plaster performance is an intrinsic property of the plaster material itself. However, transport processes are generally non-local phenomena. Therefore, it seems logical that the nature of the underlying substrate, the stone, will also influence the performance of the plaster layer. In this paper we will discuss the interaction between the substrate and the plaster layer. The focus will be on salt transport and precipitation during drying. Especially, the influence of the pore structure will be investigated.

First, we will discuss in section 2 what is known about drying and salt transport in homogeneous porous media. In section 3 a model based on invasion percolation (IP) algorithms is introduced and used to predict the drying behaviour of plaster/substrate systems. Nuclear Magnetic Resonance (NMR), our main experimental technique, is briefly discussed in section 4. In section 5 experiments on plaster/substrate systems are presented. Measurements on substrates covered with two plaster layers, potential accumulating systems, are discussed in section 6. Finally, in section 7, the conclusions are drawn.

2 Homogeneous porous media

2.1 Drying

The motions of salts through a drying porous media can only be understood when the drying process itself is understood. The drying behaviour of homogeneous porous media has been studied for many decades. Especially, isothermal drying processes driven by gradients in the vapour density have been studied in great detail both on a macroscopic and microscopic (pore-scale) level [Brakel, 1980; Le Bray 1999]. Here we briefly review the most important outcomes of all these studies.

When an object dries, water inside this object evaporates and escapes from the object as a vapour. The water can reach the external surface of this object via vapour diffusion or liquid flow. The vapour diffusion flux can be described with the following diffusion equation,

$$\vec{J}_w = -D_w \nabla \rho \quad , \quad (1)$$

where \vec{J}_w [mol/m²s], D_w [m²/s] and ρ [mol/m³] are the vapour flux, diffusion coefficient and molar density, respectively. The liquid flow can be described with Darcy's law:

$$\vec{q} = -\frac{k}{\eta} \nabla p \quad . \quad (2)$$

In this equation \vec{q} [m/s], k [m²], η [kg/ms] and p [N/m²] are the liquid volume flux, the permeability, the viscosity and the pressure. It has to be remarked that both D and k are functions of the amount of liquid water present in the system.

Generally, two drying regimes are observed, which are closely related with the two modes of transport described above. These regimes are clearly visible in NMR measurements [8], figure 1. In the first drying phase the water is rather uniform distributed over the sample. In this phase the drying rate is more or less constant, which indicates that the rate-limiting step is the vapour transport outside the porous medium. This also means that water transport goes mainly through a network of liquid water that spans the complete sample. Vapour transport is not very important in this phase. In the second drying phase a front develops, which moves into the material. During this phase the drying rate decreases and the evaporation process significantly slows down. In this phase the transport of liquid water over long distances is hindered. The water network consists of separate water clusters, which are not connected or have poor hydraulic contacts. As a consequence, water at the back of the sample cannot be transported towards the evaporation front and the clusters at the evaporation front are consumed. This results in the formation of a front. Now the rate-limiting step is the diffusion of water vapour from the drying front towards the external boundary of the object. The transition between the two drying phases is a percolation transition. The sample-spanning network breaks down in clusters with limited or no contact. This percolation process can be understood with the help of invasion percolation (IP) models [Le Bray, 1999]. In these models pores are emptied sequentially. The capillary pressure determines this sequence,

$$P_c \approx 2\sigma \cos\phi / r , \quad (3)$$

where P_c [N/m²], σ [N/m], ϕ and r [m] are the capillary pressure, the surface tension, the contact angle and the pore radius, respectively. Most building materials are water wet, which means that $\phi < 90^\circ$. During a drying process air will invade the pores with lowest entry pressure (capillary pressure), which are the widest pores. As long as there is a good hydraulic contact, these invasions will occur all over the sample (this is the first drying regime). When the network has broken down, invasion will only take place in the clusters at the evaporation front. In the case of pure water, this transition will occur when the amount of liquid water fills 20-30% of the total pore-space.

However, there are indications that salts like NaCl and NaNO₃, which are soluble up to very high concentrations, shift this transition point to much lower water contents. This indicates that these salts improve the hydraulic contacts between the separate clusters of liquid-filled pores significantly. We think that these salts promote the formation of thick water films at the pore walls and thereby facilitate liquid water flow through “empty” pores. Due to such films, separate clusters may still communicate [Yiotis, 2004].

Finally, we want to stress that it follows from equation 3 that the pore-size distribution (PSD) of a material plays a key role in the drying process. This is the main reason why we have focussed in our study of two-layer systems on the influence of the pore structure of both layers.

2.2 Salt transport and precipitation

The motion of soluble salt is closely linked with the presence of liquid water. Obviously, salt can only travel over “long distances” in the first drying phase. In the second drying phase the mobility of salt is limited by the size of the separate clusters of liquid water. In the first drying phase salt can move by diffusion and advection with the water. The relative importance of both transport mechanisms can be estimated with the so-called Peclet number [Dullien, 1991]:

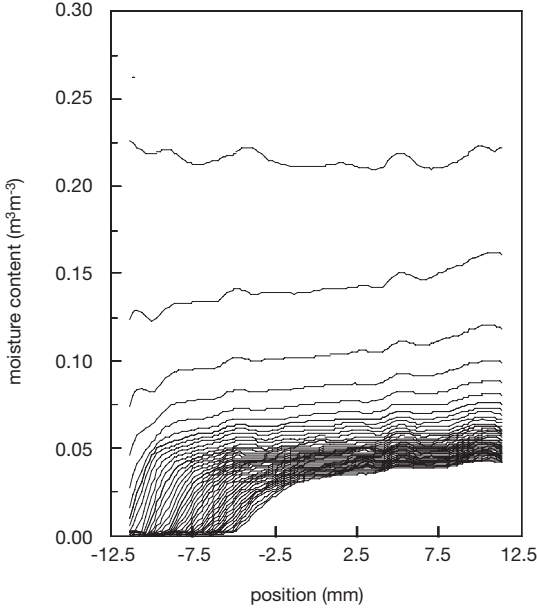


Figure 1: Moisture profiles in a fired-clay brick during a single-side drying experiment. The moisture profiles were measured with NMR [Pel, 1996].

$$Pe \equiv \frac{UL}{D_s} . \quad (4)$$

In this expression U [m/s], L [m] and D_s [m^2/s] are the absolute value of the liquid velocity, the sample size and the diffusion coefficient of salt, respectively. With help of this number two limiting cases can be distinguished: advection domination ($Pe \gg 1$) and diffusion domination ($Pe \ll 1$). In figure 2 salt profiles are shown, which illustrate both cases. The profiles were measured with NMR [Pel, 2002]. When advection dominates ($Pe \gg 1$), the salt is dragged with the water towards the evaporation front. At this front water evaporates and therefore salt accumulates. When diffusion dominates ($Pe \ll 1$), concentration differences are suppressed and the salt concentration is the same throughout the complete sample.

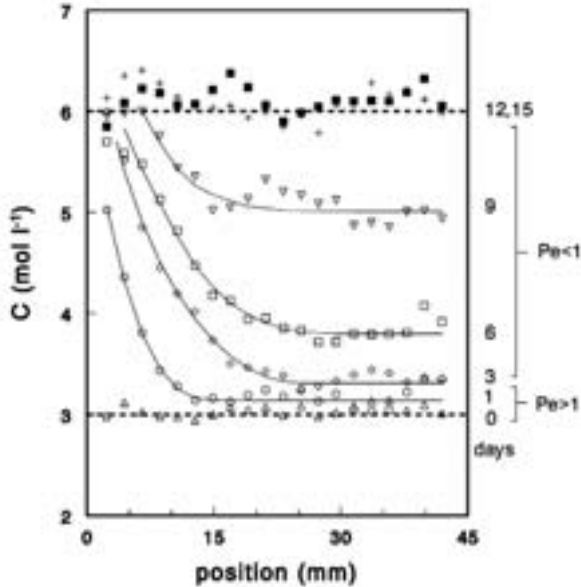


Figure 2: Na concentration profiles in a fired-clay brick during a single-side drying experiment. The concentration profiles were measured with NMR [Pel, 2002].

Due to the fact that the amount of liquid water decreases during drying sooner or later dissolved salt precipitates. When the drying process is still in the first phase, the locations where salts precipitate are related with the dominating transport mechanism. In the case that $Pe \gg 1$ salts accumulate in a narrow region close to the external boundary. At a certain moment the salt concentration exceeds the solubility limit and salts may precipitate. Therefore, we can conclude that advection dominated transport will lead to salt crystallization close to the external boundary. In the case that $Pe \ll 1$ salt will remain uniformly distributed throughout the porous medium. Due to the fact that water evaporates the salt concentration will increase. When the concentration goes over the solubility limit, salt will precipitate. In this particular case, salt crystals are formed all over the sample.

When the drying process is in its second phase, where liquid water is present in isolated clusters, salt will always crystallize in the vicinity of its host cluster. Therefore, in this phase salt crystals will be formed all over the sample.

3 Model

It has been shown that the ingress of air during a drying process obeys the rules of invasion percolation (IP) algorithms [Le Bray, 1999; Huinink, 2003]. Therefore, the first stage of the

drying process can be described completely by standard IP models. We have used IP to model the drying process in a layered structure.

The porous structure is described as a cubic network. A node in the network represents a pore with a certain radius r . In our simulations we distribute the radii according to a uniform distribution function $\alpha(r)$. In the remainder of this article or paper we will refer to the pore-size distribution with the abbreviation PSD. The PSD is defined such that,

$$\int_0^{\infty} \alpha(r) dr \equiv 1 . \quad (5)$$

The uniform distribution is given by the following expression,

$$\alpha(r) = \begin{cases} 0 & r < R - W/2 \\ W^{-1} & R - W/2 < r < R + W/2 \\ 0 & r > R + W/2 \end{cases} , \quad (6)$$

where R and W respectively are the mean and the width of the distribution. Obviously a lognormal-type of distribution is more realistic than the uniform one. Nevertheless a uniform distribution is very useful from a scientific point of view. Results generated with this distribution are much easier to interpret, which is helpful for understanding the essential physics underlying the problem. In the case that a system consists of several layers with different pore structures every layer k has its own PSD α_k characterized by a width W_k and average R_k .

The ingress of air is simulated as follows. When air invades a pore, it has to push away water. In order to do so the capillary pressure has to be overcome, see equation 3. It follows from this equation that air invades much easier large pores than small pores. Therefore, at each simulation step we search for the widest pore filled water and next to an empty pore. This pore is emptied. In this way an air cluster grows into the porous medium. At each step we check whether or not the water network completely spans the system. When this is not the case (the water is present in isolated clusters) the simulation run is ended. This point is called the fragmentation point FP. Before the FP the water network spans the complete system and salts can migrate towards the surface. After the FP water is distributed in isolated clusters and long distance migration of salt is impossible. It has to be remarked that the analogy between IP models and the drying process makes sense up to this point and therefore the model should only be used before the FP.

Finally, it has to be remarked that we do not obtain absolute timescales for drying by using the pure IP model as we do. Nevertheless the sequence in which pores are emptied is predicted correctly. In order to calculate evaporation rates one should also describe the vapour diffusion explicitly [Le Bray, 1999; Huinink, 2003].

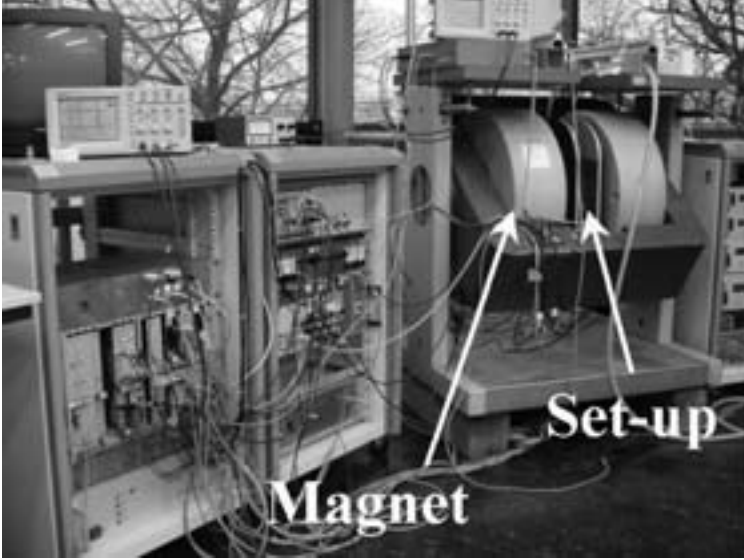


Figure 3: The NMR scanner that has been used in the research discussed in this paper. The sample is positioned in the area where the “set-up” is located, which is between the poles of the magnet.

4 Experimental methods

We have used a home built NMR scanner, which is able to probe ^1H and ^{23}Na nuclei simultaneously, figure 3. Therefore, the distribution of water and sodium salts can be measured. Here we briefly discuss the working principle. For a more detailed discussion we refer to the literature [11]. In the presence of a magnetic field all nuclei with a magnetic moment have a certain resonance frequency, which is called the Lamor frequency, ν [Hz],

$$\nu = \gamma B / 2\pi , \quad (7)$$

where B [T] and γ [Hz/T] are the magnitude of the magnetic field and the gyromagnetic ratio of the nucleus (the value of γ is different for different nuclei), respectively. By exciting the nuclei with a radio-frequency signal with a frequency equal to this Lamor frequency, the amount of nuclei can be measured. In order to be able to measure profiles, the magnetic field is tuned such that its magnitude varies linear with position:

$$B = B_0 + G(x - x_0) , \quad (8)$$

where G [T/m] and B_0 [T] are the gradient in the magnetic field, the magnitude of the field at a reference position x_0 , respectively. The measurement set-up is illustrated in figure 4 [Pel, 2002].

With the help of a step motor the sample is positioned such that the ^1H and ^{23}Na profiles can be measured at every position. At the bottom of the sample holder a vessel with a NaCl solution with a known concentration is placed, which serves as a standard. In our set-up only the Na^+ dissolved in water can be measured; crystallized salt does not contribute to the signal. The sample is only open at the topside. Dry air is blown over this side to induce drying.

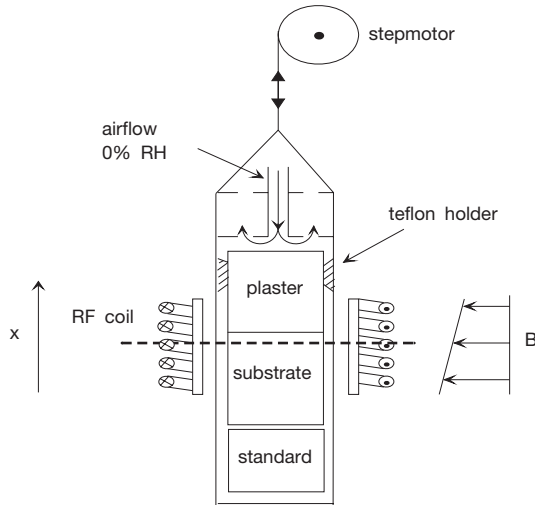


Figure 4: The experimental set-up for drying experiments. With the help of a step motor the sample is positioned such that the ^1H and ^{23}Na profiles can be measured at every position. At the bottom of the sample holder a vessel with a NaCl solution is placed, which serves as a standard. The sample is only open at the topside. Dry air is blown over this side to induce drying.

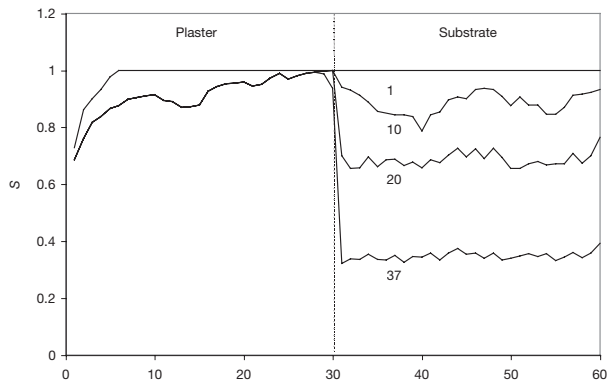


Figure 5: Saturation profiles during drying as calculated with an IP model in a plaster/substrate system in which the plaster has the smallest pores. The x -coordinate refers to a node in the network. Profiles are shown for different percentages empty pores: 1, 10, 20 and 37%.

5 Plaster/substrate systems

5.1 Model predictions

Here we present results of simulations with the model described in section 3. We focus on two extreme cases: a) the pores in the substrate are much wider than the pores in the plaster layer ($R_{sub} - W_{sub} / 2 > R_{plast} + W_{plast} / 2$) and the opposite ($R_{sub} + W_{sub} / 2 < R_{plast} - W_{plast} / 2$). In figure 5 the saturation profiles are plotted for the system in which the substrate has the widest pores. In this system air first invaded the pores in the substrate although the evaporating interface is plaster surface. The substrate is invaded first because it has the widest pores, with the lowest capillary pressure (equation 3), and therefore the least resistance against air invasion.

Results for a system in which the substrate has the smallest pores are shown in figure 6. In this particular case air first invades the plaster. Now the pores in the plaster have the lowest capillary pressure and the least resistance against air invasion.

These differences in drying behaviour will strongly influence the salt accumulation behaviour. In systems where the substrate has the widest pores, most salts will be transported from the substrate into the plaster. Most salt will end up in the plaster layer. This will not be the case when the substrate has the smallest pores. Because the plaster layer dries first all salt present in the substrate will remain in this layer. Therefore, we expect that in this particular case a lot of salt will crystallize in the substrate too.

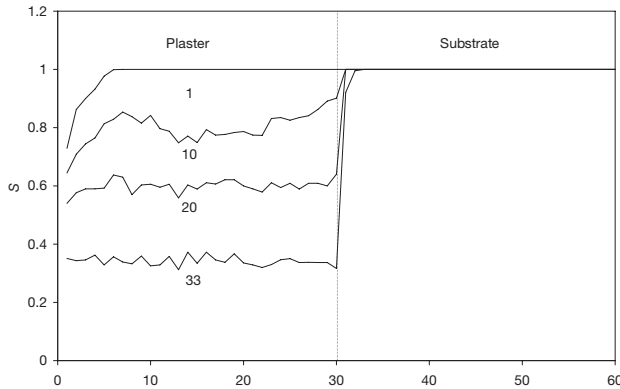


Figure 6: Saturation profiles during drying as calculated with an IP model in a plaster/substrate system in which the substrate has the smallest pores. The x-coordinate refers to a node in the network. Profiles are shown for different percentages of empty pores: 1, 10, 20 and 33%.

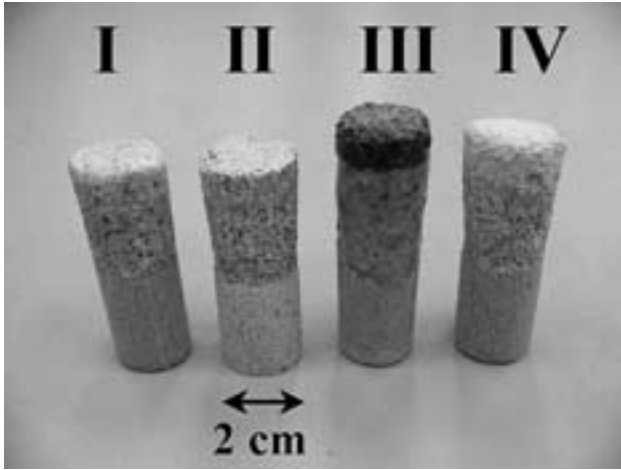


Figure 7: The samples used in the experiments. Either one (I and II) or two plaster layers (III and IV) have been applied on the substrate. Bentheimer sandstone (I, III and IV) and calcium-silicate brick (II) were used as substrates. In all cases the plaster layer adjacent to the substrate was a cement/lime/sand layer. The top-layers of the samples III and IV were a pointing mortar and gypsum-layer, respectively.

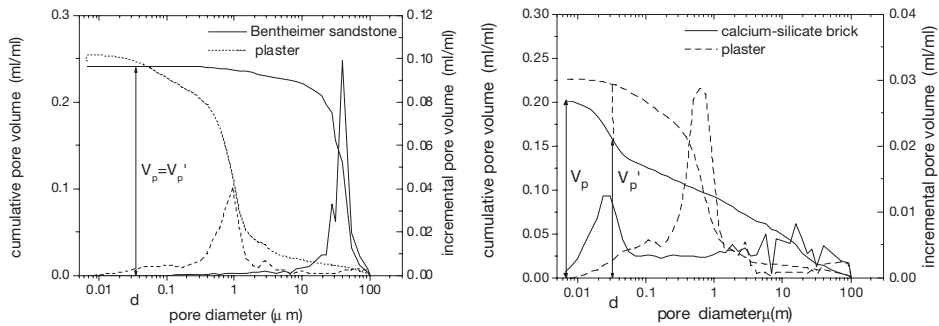


Figure 8: The pore-size distributions (PSD) of the plaster/Bentheimer (left) and plaster/calcium-silicate (right) two-layer systems. These curves have been measured with mercury intrusion porosimetry (MIP). The solid lines represent the PSD of the substrates (Bentheimer or calcium-silicate). The dashed lines are the curves of the plaster layer.

5.2 Experiments

5.2.1 Materials

In order to investigate the influence of the pore-structure on salt transport and accumulation in two-layer systems, we have applied the same plaster on two different substrates (I and II in figure 7). The plaster was made of lime, cement and sand in the ratio 4:1:10 (v/v). As substrates

we have chosen a Bentheimer sandstone (I) and a calcium-silicate brick (II). In the rest of this paper we will refer to these systems with B (Bentheimer) and CS (calcium-silicate brick). These substrates have completely different pore-size distributions, which is illustrated in figure 8. The PSD of the plaster is peaked around $1\ \mu\text{m}$, but has long tails. The Bentheimer has a very narrow PSD, peaked around $50\ \mu\text{m}$. The calcium-silicate has a very wide PSD. It has a significant amount of pores with very small sizes ($\sim 20\ \text{nm}$). It has also a fraction of very big pores ($> 10\ \mu\text{m}$). The important point is that the pores of the plaster are smaller than the pores in the Bentheimer, but they are bigger than an important fraction of the pores in the calcium-silicate.

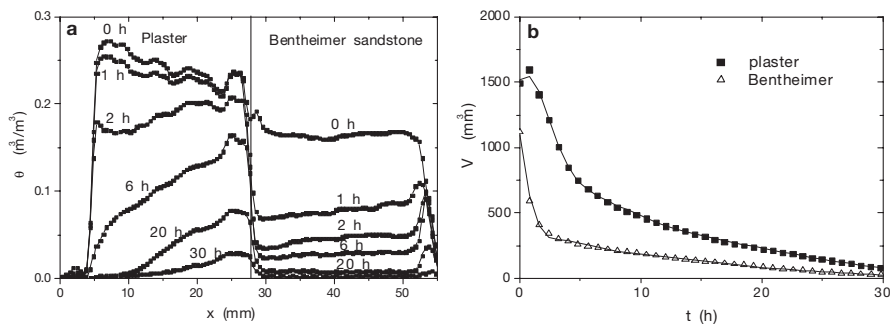


Figure 9: The drying of a Bentheimer/plaster system saturated with pure water. The water profiles (left) and the total amounts in the plaster and the substrate (right) are shown. The topside, where water could escape the sample, was located at the air/plaster interface.

5.2.2 Pure water

First the drying behaviour of the two systems has been measured in the absence with salt. The topside, where water could escape from the sample, was in both systems located at the air/plaster interface. Results for the Bentheimer/plaster system are shown in figure 9. In figure 9 the water profiles are shown and the total amounts in the Bentheimer and the plaster layer. Although the Bentheimer is located at the back of the sample, air first invades this layer. In a later stage the plaster layer also starts to dry. At low moisture contents in the plaster a front is formed in the plaster, which moves into this layer. The formation of this front indicates that the liquid water is distributed in separate cluster with limited hydraulic contact. The drying behaviour of the calcium/silicate system is completely different, see figure 10. The most important difference is the fact that in CS system the plaster layer dries out first. After 40 h the substrate still contains a significant amount of water, while the plaster is nearly dry. The drying behaviour of both systems can be understood from their PSD, figure 8. As we have discussed in section 2.1 the first pores that are emptied during a drying process are the pores with the lowest capillary pressure, which are according to equation 3 the widest pores. In the B system the widest pores are located in the substrate. This explains why air first invades the Bentheimer and

later the plaster. It also explains why the substrate of the CS system still contains a lot of water, while the plaster is nearly dry. The substrate, a calcium-silicate brick, has many small pores. These small pores are not easily invaded by air due to the high capillary pressures. Therefore, water will remain as long as possible in these pores and the substrate will contain a lot of water.

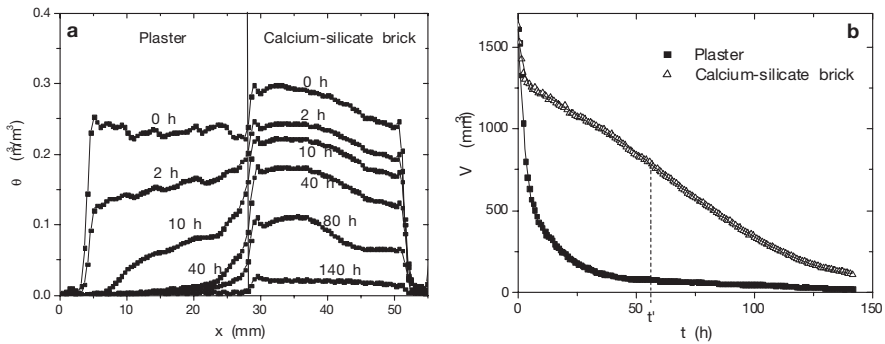


Figure 10: The drying of a calcium-silicate/plaster system saturated with pure water. The water profiles (left) and the total amounts in the plaster and the substrate (right) are shown. The topside, where water could escape the sample, was located at the air/plaster interface.

5.2.3 Salt solutions

We have also studied the drying behaviour of the same systems in the presence of salt. Both systems were saturated with a 4 M NaCl solution. Again the topside, where water could escape from the sample, was located at the air/plaster interface. The water and the dissolved Na were measured. In section 5.2.5 we will discuss Na-behaviour during this experiments. Here we focus on the transport of the water.

In figure 11 the water profiles and the total amounts of water during drying are shown for the B system. As in the absence of salt air first invades the Bentheimer substrate and later on the plaster. However, remarkable differences between the drying in the presence (figure 11) and absence (figure 9) are observed. First of all, salt slows down the drying process. Due to the presence of salt the equilibrium relative humidity of liquid water decreases. As a consequence the driving force for the evaporation process, a gradient in relative humidity over the external boundary layer, decreases. Secondly, salt suppresses the formation of a drying front even in the late stage of the drying process. Although, the liquid water is distributed in separate clusters of pores, these clusters can easily exchange water. They stay in good hydraulic contact, which might indicate that salt could promote the formation of thick wetting films.

In the case of the CS system salt seems to affect the drying process in a similar fashion, figure 12. As in the presence of pure water, figure 10, the calcium-silicate substrate still contains a lot of water, when the plaster is nearly dry. The main influence of salt is again on the drying rate, which is reduced, and the drying front, which is suppressed.

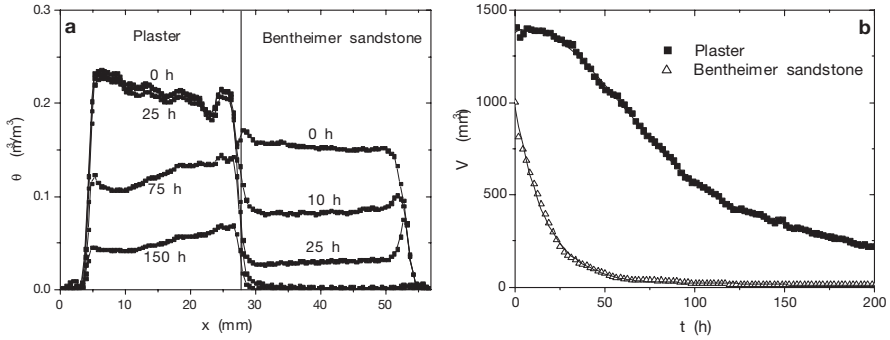


Figure 11: The drying of a Bentheimer/plaster system saturated with a 4 M NaCl solution. The water profiles (left) and the total amounts of water in the plaster and the substrate (right) are shown. The topside, where water could escape the sample, was located at the air/plaster interface.

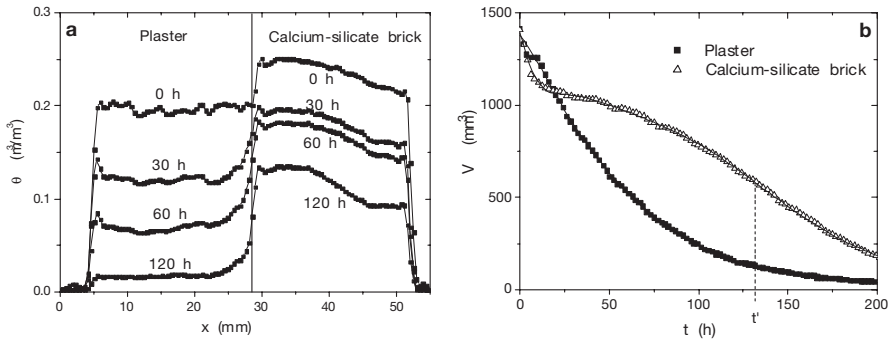


Figure 12: The drying of a calcium-silicate/plaster system saturated with a 4 M NaCl solution. The water profiles (left) and the total amounts of water in the plaster and the substrate (right) are shown. The topside, where water could escape the sample, was located at the air/plaster interface.

5.2.4 Substrate influence

From our drying experiments we can already conclude that the transport and accumulation of salts will not solely depend on the plaster properties. It was observed that the order in which layers are invaded by air during the drying process is strongly influenced by the substrate. Although, the same plaster was used the drying of the system as a whole was significantly modified by the characteristics of the substrate. To be more precise, the difference in the pore structure between the plaster and the substrate is a key parameter. When the plaster has small pores compared to the substrate, the substrate will dry out while the plaster still contains a lot of water. In this case we expect that salts will be dragged into the plaster. Therefore, we expect accumulation of salts at the plaster/air interface, the external surface of the system. When the plaster has large pores compared to the substrate, the plaster will dry out first. In this particular case, we expect that much salt will

stay in the substrate and precipitate in the substrate. Therefore, we expect that the performance of a plaster is closely related with the properties of the substrate on which it is applied.

5.2.5 Salt transport and accumulation

In section 5.2 we have discussed the drying behaviour of the B and CS system in the presence of salt. In this experiments we have also measured the amounts of Na dissolved in water. In figure 13 the Na profiles and Na amounts are shown for the B system. In the first 25 hours the amount of salt in the Bentheimer layer decreases, while it increases in the plaster. The formation of a peak in the plaster layer indicates that advection is in the phase the dominant transport process for salt. In this period air invades the substrate and water flows from the substrate to the plaster, where it evaporates at the air/plaster interface. Along with the water salt is dragged from the substrate into the plaster. The peak grows until the salt solution is saturated. From this point on salt crystallizes. It follows from the Na-profiles that the salt initially crystallizes at the external surface. In the late stage of the drying process, the Na profiles in the plaster are uniform and salt crystallization will occur everywhere in the plaster layer. The important point is that the NMR data suggest that most salt will precipitate in the plaster layer and not in the substrate.

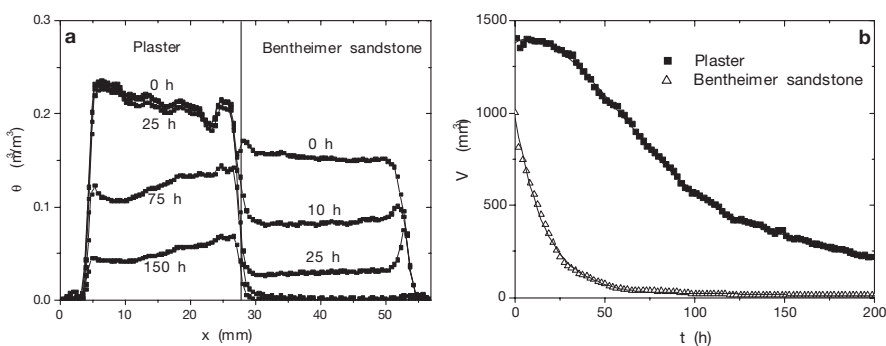


Figure 13: The behaviour of dissolved Na during the drying of a Bentheimer/plaster system saturated with a 4 M NaCl solution. The Na profiles (left) and the total amounts of Na in the plaster and the substrate (right) are shown. The topside, where water could escape the sample, was located at the air/plaster interface.

At the end of the drying process we have cut the sample in slices and analysed it with the help of ion-chromatography (IC). With this method the total amount of salt (dissolved and precipitated) can be determined. Results are plotted in figure 14. This plot confirms that most salt has been transported from the Bentheimer to the plaster layer. The salt distribution is peaked at the external surface (the plaster/air interface), which can be explained by the fact that in the beginning of the drying process a concentration peak has develop at the surface, see figure 13. In figure 15 the Na profiles and Na amounts are shown for the CS system. The sodium profiles

seem to follow the drying profiles (figure 12). Overall the Na-signal decays much faster in the plaster layer than in the calcium-silicate brick. The signal decay in the plaster layer could indicate that either salt precipitates or it is transported to the substrate.

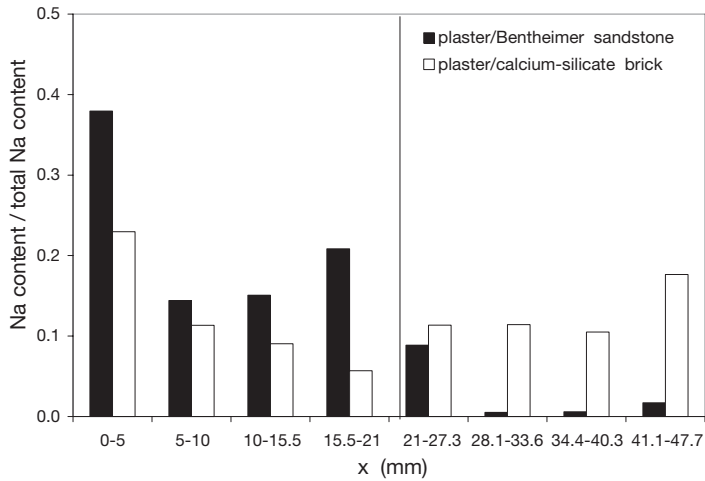


Figure 14: The salt distribution at the end of the drying process as measured with ion-chromatography. The left part of the plot is the plaster layer and the right part the substrate.

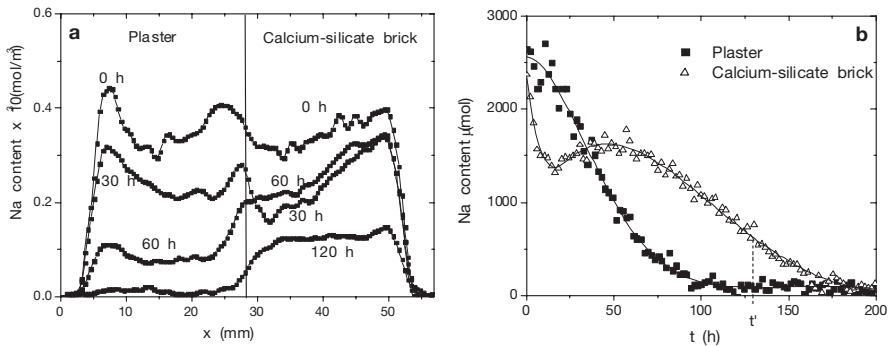


Figure 15: The behaviour of dissolved Na during the drying of a calcium-silicate/plaster system saturated with a 4 M NaCl solution. The Na profiles (left) and the total amounts of Na in the plaster and the substrate (right) are shown. The topside, where water could escape the sample, was located at the air/plaster interface.

Because we do not observe a significant increase of the Na signal in the substrate, we attribute the signal decay in the plaster to salt crystallization. From both the moisture and salt profiles it can be concluded that initially most salt will precipitate in the plaster. In the later stage of the drying

process when the plaster layer is nearly dry, salt will precipitate in the calcium-silicate substrate. This is confirmed by IC measurements, see figure 14. Salt has crystallized everywhere in the sample. Both the NMR and IC measurements indicate that the drying process determines the process of salt accumulation. When a substrate has wider pores than the plaster (B system), the substrate will dry out first and nearly all salt will precipitate in the plaster near the external surface. When the substrate has a significant amount of small pores, the plaster will be dry first. In this case salt crystals will form both in the plaster and the substrate.

6 Two plaster layers on a substrate – experiments

6.1 *Accumulating plasters – the concept*

Two main categories of the salt resistant plasters exist: transporting and accumulating plasters [12]. Generally, the accumulating type is achieved by applying a water repellent agent on the finishing plaster layer. It prevents water and salt penetration into the surface layer and salt accumulates in the base layer of the plaster near to the substrate. The base layer should have a big porosity, allowing salts to crystallize without causing damages. In the present research we investigate if plaster without a water repellent additive but with two layers having different pore sizes could behave as accumulating system. The idea behind this concept is based on drying theory, in which the moisture transport is related to the capillary pressure and the pore sizes of the materials. Generally, moisture and therefore salt will remain in the material with the smallest pores. Therefore, an accumulating plaster could be made by using a base plaster layer with pore sizes an order of magnitude smaller than the pore sizes of the surface plaster layer and the substrate. First, we discuss a few predictions done with the help of the IP model. Secondly, we present results of NMR measurements on these type of systems.

6.2 *Model predictions*

In principle three extreme cases can be distinguished: the widest pores are either in the top layer, base layer or substrate. In fact the last case has been discussed in section 5.1.2. From that discussion we can already conclude that these system will never be able to act as an accumulating system. All salts present in the substrate will be transported towards the top layer. Calculations have been performed with the same algorithms as used in our plaster/substrate study; for a description of the model we refer to section 3. Simulations were performed up to the point where the system no longer contains a sample-spanning network of water, the fragmentation point FP.

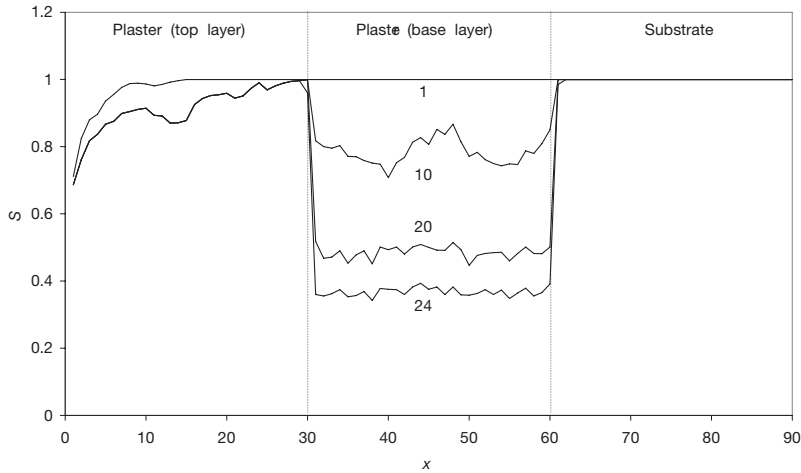


Figure 16: Saturation profiles during drying as calculated with an IP model in a system with two plaster layers on top of substrate. The x -coordinate refers to a node in the network. The base layer has the widest pores. Profiles are shown for different percentages empty pores: 1, 10, 20 and 24%.

First we have studied a system in which the widest pores are in the base layer of the system. Saturation profiles are plotted in figure 16. The system behaves as expected: air first invades pores in the central layer, which have the lowest capillary pressure to resist, see equation 3. We expect that in this system salts present in the substrate will remain in the substrate. Due to the fact that the central layer dries out first until the fragmentation point, there is no hydraulic contact between substrate and the plasters layers in the rest of the drying process.

We have also studied a system in which the widest pores are located in the top layer, see figure 17. Here we observe that first the top layer dries out. This has important implications for the salt present in the substrate. Depending on the difference in pore sizes between the base layer and the substrate salt either accumulates in the base layer or stays in the substrate. This suggests that the ideal accumulating systems should obey the following relation:

$$R_{base} < R_{substrate} < R_{top}. \quad (9)$$

When this relation is satisfied most salt present in the substrate will end up in the base layer.

6.3 Experimental results

6.3.1 Materials

Two systems have been made, which are identical except for the top layer, see figure 7. In both systems the substrate is Bentheimer sandstone and the base-layer is a lime/cement plaster. On one system a gypsum layer has been applied (IV). The other system was covered with a coarse

layer of pointing mortar (III). Both systems are of little practical value, but may have the right drying behaviour. In the remainder of this report we will refer to both systems as the gypsum and pointing mortar systems.

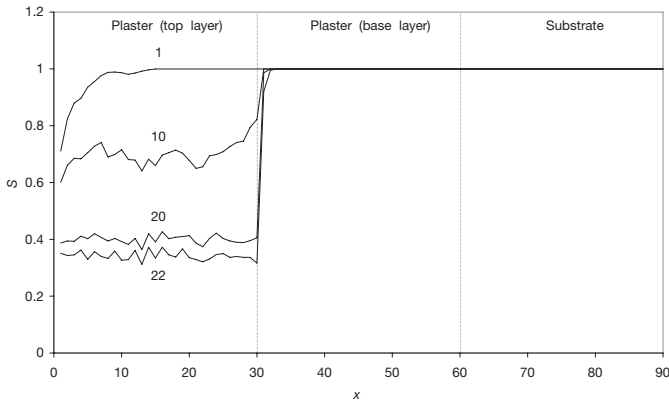


Figure 17: Saturation profiles during drying as calculated with an IP model in a system with two plaster layers on top of substrate. The x -coordinate refers to a node in the network. The top layer has the widest pores. Profiles are shown for different percentages empty pores: 1, 10, 20 and 22%.

Sample III

Substrate: Bentheimer sandstone
 Base layer: Lime / Cement
 Top layer: Pointing mortar

Sample IV

Substrate: Bentheimer sandstone
 Base layer: Lime / Cement
 Top layer: Gypsum

6.3.2 Pointing mortar as top layer

Although, a pointing mortar is useless as a plaster material it at least helps us to test the concept of an accumulating plaster, because the condition 9 is satisfied. Drying experiments have been performed on a sample saturated with pure water. In figure 18 the water profiles are shown. The drying behaviour is as expected: the top layer quickly dries out first. Then the substrate starts to dry. When the substrate is nearly dry, the base-layer starts drying.

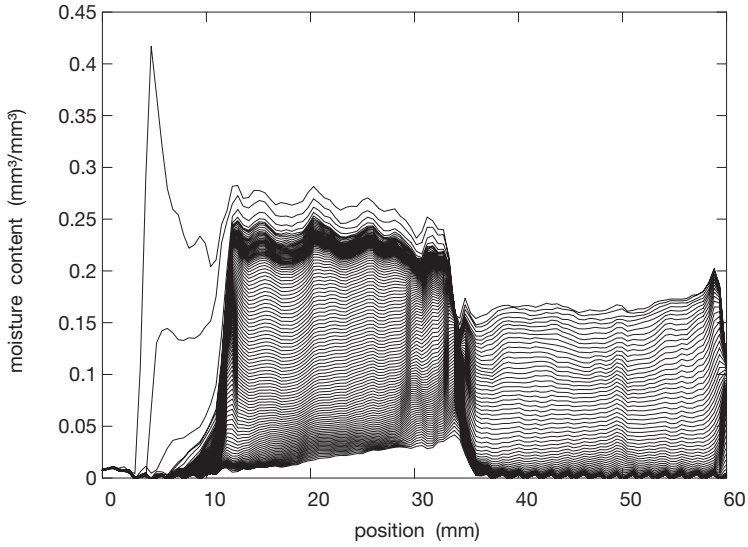


Figure 18: Water profiles during drying of a system with pointing mortar as the top-layer that was saturated with pure water. The top-layer is located at $x = 4$ mm.

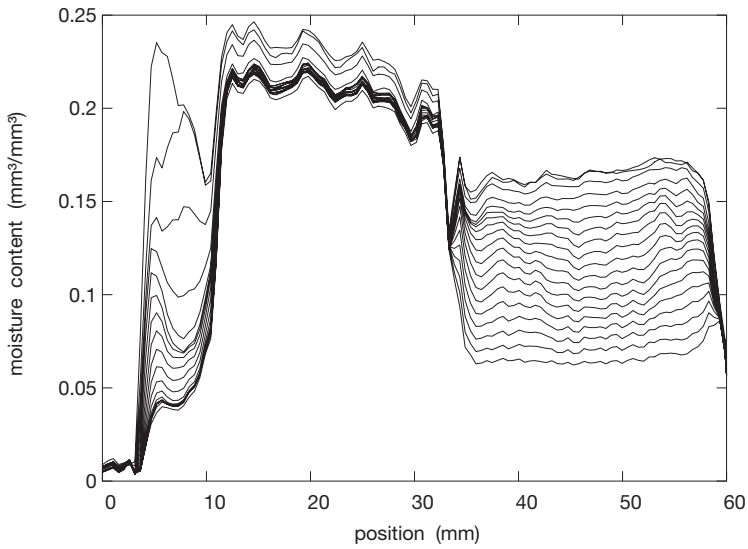


Figure 19: Water profiles during drying of a system with pointing mortar as the top-layer that was saturated with 4 M NaCl solution. The top-layer is located at $x = 4$ mm.

We have also performed drying experiments on the same sample but now it was saturated with a 4 M NaCl solution instead of pure water. Drying profiles are shown in figure 19. The drying behaviour is significantly modified by the presence of salt. The most remarkable feature is the fact

that the salt changes the drying of the top-layer. As in the absence of salt (figure 18) the top-layer quickly dries in the beginning of the process. However, the drying of this top-layer significantly slows down at a certain moment. As a result, the top-layer still contains a reasonable amount of moisture when the substrate starts to dry.

This will have important consequences for the accumulation capabilities of this system. Due to the presence of salt the drying properties of the top-layer are modified such that hydraulic contact between the external surface and important parts of the system is established during a long period. Due to this hydraulic contact salts easily migrate to the external surface and will accumulate at the outer surface of the system. This has important implications for our application. It seems that salt is able to modify the properties of the system such that pore-size differences no longer determine the complete process. Therefore, we conclude that it is not possible to make a salt-accumulating system purely based on contrasts in the pore-sizes between the different layers.

6.3.3 *Gypsum as top layer*

Drying experiments have been performed on a sample saturated with pure water. In figure 20 the water profiles are shown. The top-layer and the substrate dry more or less simultaneously. The base-layer is still wet when the top-layer and the substrate are nearly dry. Already on the basis of this drying behaviour it can be argued that the system will not have very good accumulating properties. In the case of the pointing mortar (section 3.1) the drying of the substrate and the top-layer did not occur simultaneously and the top-layer dried out first. This is not the case in this particular sample.

We have also performed drying experiments on the same sample but now the sample was saturated with a 4 M NaCl solution instead of pure water. Drying profiles are shown in figure 21. The drying behaviour is significantly modified by the presence of salt. The most remarkable feature is the fact that salt changes the drying of the top-layer. As in the absence of salt (figure 20) the top-layer and substrate dry simultaneously in the early stages of the drying process. However, the drying of this top-layer significantly slows down at a certain stage. As a result, the top-layer still contains a reasonable amount of moisture when the substrate is nearly dry. Already on the basis of the drying behaviour in the absence of salt we argued that this system could not have very good accumulating properties. The salt seems to worsen it even more. The properties of the top-layer are modified such that hydraulic contact between the external surface and important parts of the system is established during a long period.

Due to this hydraulic contact salts easily migrate to the external surface and will accumulate at the outer surface of the system. This has important implications with respect to our application. It seems that salt is able to modify the properties of the system such that pore-size differences no longer determine the complete process. Again we conclude that it is not possible to make a salt-accumulating system purely based on contrasts in the pore-sizes between the different layers.

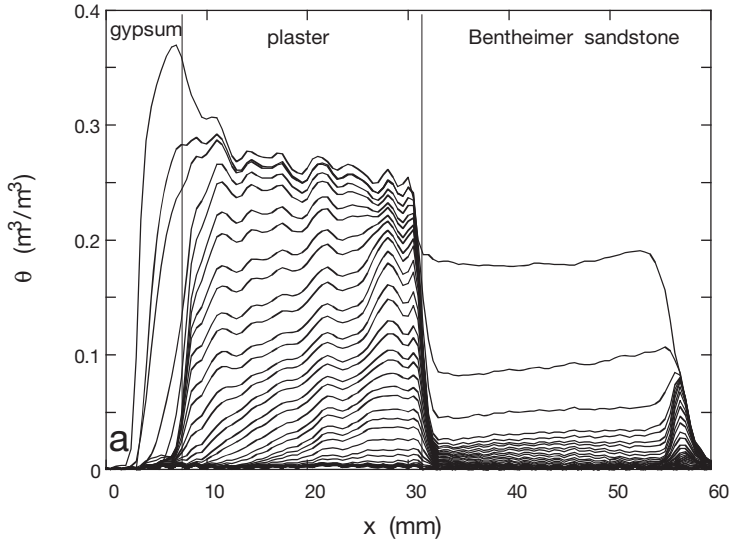


Figure 20: Water profiles during drying of a system with gypsum as the top-layer that was saturated with pure water. The top-layer is located at $x = 3$ mm.

7 Conclusions

- A. In this study we have shown that the transport and accumulation of salt is not a material property of the plaster. This process is strongly influenced by the properties of the underlying substrate. Therefore, the performance of a plaster should always be evaluated together with the substrate of interest.
- B. When a plaster is applied on a stone with wider pores than the plaster, salts will accumulate in the plaster (especially close to the plaster/air interface). This is due to the fact that first the stone dries out. Along with the water most salt is transported from the substrate to the plaster. In the case that a plaster is applied on a stone with a significant fraction of smaller pores than the plaster, salt crystals will be distributed more equally over both layers. First the plaster layer dries out and salts precipitate in this layer. Later the substrate dries and salt crystallizes in this layer.
- C. What accumulation behaviour is preferable is an open issue. From a mechanical point of view it seems to be better to choose for a system that tends to spread out the crystals as much as possible in space, which will avoid stress localization. Following this reasoning a plaster should be chosen that dries faster than the substrate (a CS-type system). However, if avoiding damage on the substrate is the main target, then the substrate should dry faster than the plaster (a B-type system).

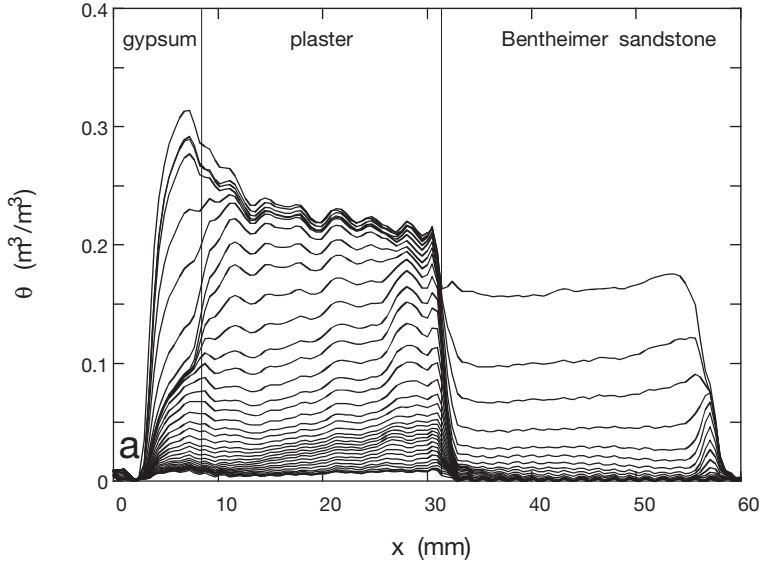


Figure 21: Water profiles during drying of a system with gypsum as the top-layer that was saturated with 4 M NaCl solution. The top-layer is located at $x = 3$ mm.

- D. We have put forward a concept for an accumulating system based on difference in pore sizes. Two plaster layers should be applied on top of a substrate. The base layer should have smaller pores than the substrate. The top layer should have the wider pores than the substrate.
- E. The drying behaviour in the absence of salt of the proposed systems seems to justify the concept.
- F. However, in the presence of salt the drying behaviour of the systems was modified in such way that the accumulating performance of these systems seems to be lower. Salt prevents the top layer to dry out fully. Therefore, these systems still might act as transporting systems.

Acknowledgement

This work was financially supported by the European Union and has been carried out in the COMPASS project. We thank Tomas Wijffels (TNO) for preparing the samples.

References

- Brakel, J. van (1980) 'Mass transfer in convective drying', *Advances in Drying*, Vol. 1, pp. 217.
- Callaghan, P.T. (1991) *Principles of Nuclear Magnetic Resonance Microscopy*, Oxford, Clarendon Press.
- Charola, A.E.(2000) 'Salts in the deterioration of porous materials: an overview', *Journal of the American Institute for Conservation*, Vol. 5, pp. 327-343.
- Dullien, F.A.L.(1991) *Porous media: fluid transport and pore structure*, London, Academic Press.
- Evans, I.S.(1970) 'Salt crystallization and rock weathering: a review', *Revue de Geomorphologie dynamique*, Vol. 19, pp. 153-177.
- Goudie, A.S. and Viles, H.(1997) *Salt Weathering Hazards*, Chichester, Wiley.
- Huinink, H.P., Pel, L. and Michels, M.A.J.(2002) 'How ions distribute in a drying porous medium: a simple model', *Physics of Fluids*, Vol. 14, pp. 1389-1395.
- Huinink, H.P., Pel, L. and Michels, M.A.J. (2003) 'The structure and transport properties of liquid clusters in a drying porous medium, *Physical Review E*, 68, pp. 56114.
- Le Bray, Y. and Prat, M.(1999) 'Three dimensional pore network simulation of drying in capillary porous media', *International Journal of Heat and Mass Transfer*, Vol. 42, pp. 4207-4224.
- Pel, L., Brocken, H. and Kopinga, K.(1996) 'Determination of moisture diffusivity in porous media using concentration profiles', *International Journal of Heat and Mass Transfer*, Vol. 39, pp. 1273-1280.
- Pel, L., Huinink, H.; Kopinga, K. (2002) 'Ion transport and crystallization in inorganic building materials as studied by nuclear magnetic resonance', *Applied Physics Letters*, Vol. 81, pp. 2893-2895.
- Wijffels, T.J., Groot, C.J.W.P. and Hees, R.J.P. van (1997) *Performance of restoration plasters*, Proc. 11th Int. Brick/Block Masonry Conf., Shanghai, China, pp. 1050-1062.
- Yiotis, A.G., Boudouvis, A.G., Stubos, A.K., Tsimpaniogiannis, I.N. and Yortsos, Y.C. (2004) 'Effect of liquid films on the drying of porous media', *AIChE Journal*, Vol. 50, pp. 2721-2737.